

The need for “objective measurements” in FDG and amyloid PET neuroimaging

Daniela Perani · Leonardo Iaccarino ·
Valentino Bettinardi

Received: 27 March 2014 / Accepted: 21 July 2014 / Published online: 5 August 2014
© Italian Association of Nuclear Medicine and Molecular Imaging 2014

Abstract The process leading to the identification and validation of biomarkers for the diagnosis of early Alzheimer’s disease (early AD) has been a major focus of research interest in the past 10 years, and has been accompanied by a debate on the feasibility of implementing the research criteria in clinical practice. In the context of imaging performed using the two currently identified classes of AD biomarkers, i.e. markers of pathology and neurodegeneration, amyloid PET and ^{18}F -FDG PET imaging are decisive tools whose crucial value is acknowledged in the recent guidelines for the early diagnosis of AD and other dementia conditions. The available recommendations draw on an extensive body of PET imaging literature, based mainly on visual methods. For the research criteria to be adopted in clinical settings, several uncertainties and gaps in knowledge must be overcome, in particular the low sensitivity and specificity provided by visual qualitative PET scan evaluation at the single-subject level. Indeed, the sensitivity and specificity of the ^{18}F -FDG PET methods depend largely on the use of “objective methods” that result in improved accuracy for diagnosis and prognosis. Here, we review the most widely used parametric and semi-quantitative approaches to ^{18}F -FDG

PET and amyloid PET imaging, highlighting their importance in early and differential diagnosis in both research and clinical settings.

Keywords Quantification · Quantitative analysis · Parametric analysis · Partial volume effects · Amyloid · ^{18}F -FDG-PET

Introduction

The process leading to the identification and validation of biomarkers for the diagnosis of early Alzheimer’s disease (early AD) has been a major focus of research interest in the past 10 years [1] and has been accompanied by a debate on the feasibility of implementing the research criteria [2] in clinical practice. Evidence supporting the validity of biomarkers is now accumulating and standardization procedures are under development by European and US working groups, thus making biomarkers increasingly prominent in the clinical diagnosis and management of AD and related dementias [1]. Both the IWG and the NIA-AA criteria state that individuals with progressive cognitive impairment who are positive for specific AD biomarkers have high odds of carrying AD pathology [2].

It is now clear that positron emission tomography (PET) imaging can improve the early diagnosis of AD and the differential diagnosis of dementias [3]. The importance of identifying individuals at risk of developing dementia among people with subjective cognitive complaints or mild cognitive impairment (MCI) has clinical, social and therapeutic implications [4]. In the context of imaging performed using the currently identified classes of AD biomarkers, i.e. markers of pathology and neurodegeneration, amyloid PET and ^{18}F -FDG PET imaging are decisive

Color figures online at <http://link.springer.com/article/10.1007/s40336-014-0072-0>

D. Perani · L. Iaccarino · V. Bettinardi
Division of Neuroscience, Nuclear Medicine Department,
San Raffaele Hospital, Milan, Italy

D. Perani (✉) · L. Iaccarino
Division of Neuroscience San Raffaele Scientific Institute,
Nuclear Medicine Department San Raffaele Hospital,
Vita-Salute San Raffaele University, Via Olgettina 60,
20132 Milan, Italy
e-mail: perani.daniela@hsr.it

tools, whose value is acknowledged in the recent guidelines for the early diagnosis of AD and other dementia conditions [5]. The available recommendations, however, draw on an extensive body of PET imaging literature based on visual methods; such methods show limited sensitivity and specificity and fail to provide a clear cut-off between normal and pathological findings [3]. Thus, for the criteria to be adopted in clinical settings, several uncertainties and gaps in knowledge must be overcome. A major issue is the low sensitivity and specificity provided by visual qualitative PET scan evaluation at the single-subject level. The sensitivity and specificity of ^{18}F -FDG PET depend largely on the use of “objective methods”, resulting in improved diagnostic and prognostic accuracy. These methods can be “absolute” or “relative”, involving, respectively, quantification based on concomitant arterial blood sampling, or on reference values (e.g. the reference region approach). Reference-based measurements are the choice for the majority of clinical PET centers as they are less invasive and less uncomfortable for the patient (reducing scanning time, avoiding continuous blood sampling, etc.).

The aim of this review is to provide useful insights into the advantages (in terms of diagnostic accuracy) of semi-quantitative measurements in clinical settings. In the context of ^{18}F -FDG PET imaging, scan reporting is routinely based on visual analysis of brain metabolic patterns and asymmetries by an expert reader. As outlined by the US Society of Nuclear Medicine and the European Association of Nuclear Medicine [6], the time has come for efforts to make readouts standardized and based on operator-independent analyses. ^{18}F -FDG PET images can be assessed, using parametric or voxel-wise analyses, by comparing the

subject’s scan with normative data from healthy controls (HCs). Parametric analysis tools can be divided into two categories: voxel-based mapping tools and summary metrics of temporoparietal hypometabolism. Voxel-based mapping tools are topographical voxel-by-voxel estimates of the departure of metabolism from a data set of normal scans. Several automated or semi-automated tools are available, either free of charge (such as statistical parametric mapping—SPM, three-dimensional stereotactic surface projections—SSP and Neurostat[®], AD-related hypometabolism convergence index—HCI) or for a fee (such as BRASSTM, <http://www.hermesmedical.com>, PMOD[™] with PALZ algorithm, and Neurogam[™]). Some of the procedures implemented in these tools have been validated in dementia conditions [7–10]. The resulting maps provide detailed anatomical localizations of dysfunctional brain regions, thereby allowing much greater sensitivity and specificity [11] (see Fig. 1). As regards amyloid PET, the development of new radiotracers, currently at various stages of FDA evaluation and approval, has brought amyloid imaging to the threshold of clinical use [12]. There is, however, a great concern over how a dichotomous visual readout (positive or negative amyloid PET) might be used (or misused) in the diagnostic process. This is a key issue involving both nuclear medicine specialists and clinicians. Crucially, to prevent a positive amyloid scan from becoming a de facto diagnosis of AD, proper analyses and recommendations are necessary. Semi-quantitative measures (such as the standardized uptake value ratio—SUVr, or the distribution volume ratio—DVR) or automated readouts (such as those obtained using SPM-based protocols) have the advantage of being

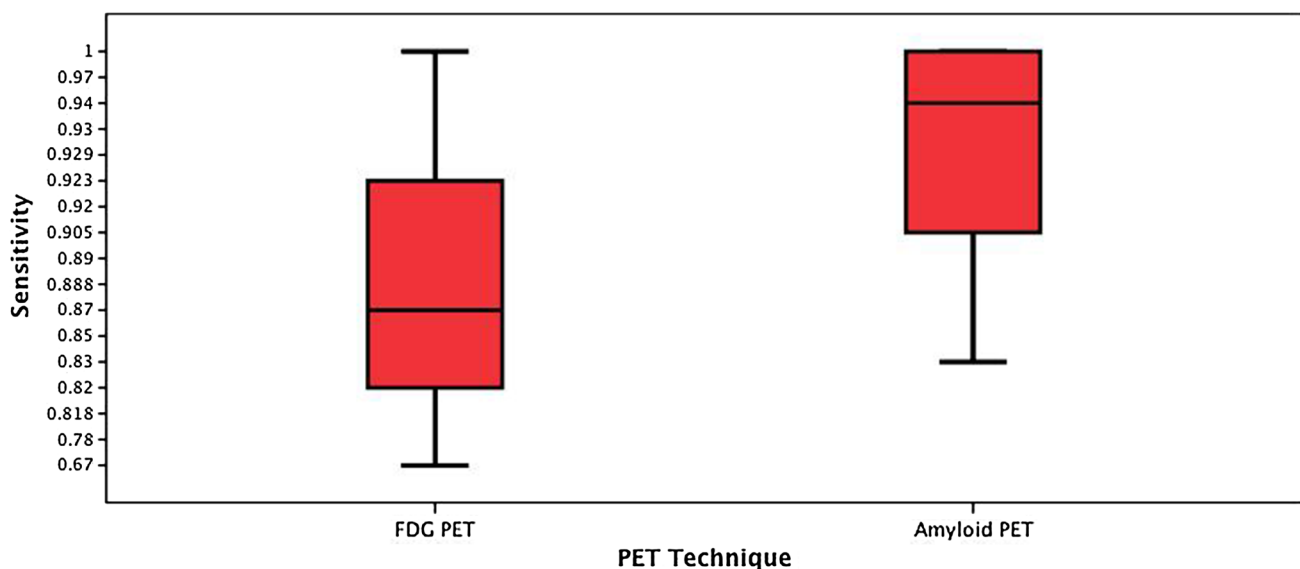


Fig. 1 Sensitivity of the ^{18}F -FDG and amyloid PET studies included in the survey of the literature by Perani et al. [11] (color figure online)

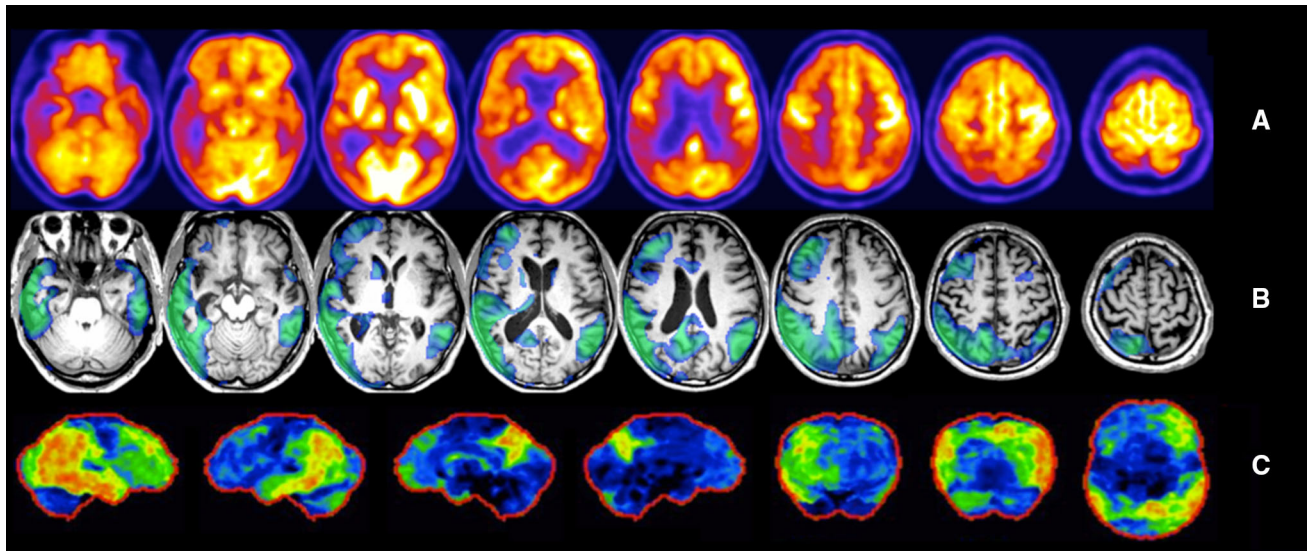


Fig. 2 ^{18}F -FDG PET images in a patient with FTD. **a** ^{18}F -FDG distribution map, **b** ^{18}F -FDG SPM-t map, **c** ^{18}F -FDG NeurostatTM 3D-SSP map (Courtesy of Drs. D. Chan, K. Moodley, L. Minati, Brighton and Sussex University Hospital, UK) (color figure online)

operator independent. Semi-quantitative approaches strictly require thresholds for positivity/negativity. Thresholds are necessary for several reasons: (1) to allow comparison with pathological conditions; (2) to allow equalization across different ligands; (3) to provide estimation of the risk of developing dementia. In addition, major caveats in amyloid quantification approaches could affect the measurements and therefore need to be taken into account. Examples include partial volume errors or specific-radioligand characteristics such as flow dependence. Quantitative amyloid measures will be of utmost value in the preclinical AD phase to discriminate ‘accumulators’ from ‘non-accumulators’, a distinction that in normal individuals could predict the development of MCI (which can be a prodromal stage of AD) into full-blown AD.

On the basis of a recent and extensive survey of the relative literature it was concluded that both topographical and pathological PET markers are very accurate and sensitive to early diagnosis of AD, as well as to differential diagnosis with other forms of dementia [e.g. the frontotemporal dementia (FTD) spectrum or dementia with Lewy bodies (DLB)], when parametric approaches are used [11].

^{18}F -FDG PET measures

Traditionally, routine clinical PET examinations are evaluated and assessed visually by trained physicians, whose aim is to detect asymmetries or abnormalities in ^{18}F -FDG uptake across the brain. This approach is heavily dependent on personal expertise and on other confounding variables like inter-individual anatomical differences and atrophy across different patients, which may limit the agreement

between different raters. Obviously, in clinical settings, absolute quantification of ^{18}F -FDG glucose consumption requiring arterial sampling cannot be recommended on account of the discomfort to patients due to the invasive nature of this approach. Relative measurements of ^{18}F -FDG PET data, based on voxel-based analyses (such as NeurostatTM based on 3D-SSP, the AD-related t-sum index in the PALZ algorithm of PMOD, SPM, HCl, etc.), yield observer-independent results (see Fig. 2), which are highly valuable for single-subject PET analysis, improving diagnostic accuracy in clinical settings [1, 9] (see below for details). As we highlighted in our recent survey [11], there are currently only a few papers in the literature regarding the increased diagnostic value of semi-quantitative methods in ^{18}F -FDG PET [13–16]. However, recent advances in the development of algorithms and programs for analyzing PET images are changing this situation.

Foster et al. [13], in their systematic work, showed an overall accuracy increase (84–89 %) when adopting 3D-SSP measurements rather than qualitative visual evaluations. The modest size of this improvement can be attributed to the fact that the raters involved in the visual evaluation were very skilled and expert, which (unfortunately) may not always be the case [13]. Patterson et al. [14] showed that the early detection of MCI patients at risk of developing AD was better when using SPM ($N = 18$) than when using visual evaluation ($N = 11$) in a total of 30 MCI subjects followed up for 3 years [14]. Also, Rabino-vici et al. [15] recently showed that the adoption of semi-quantitative measurements of ^{18}F -FDG PET increased specificity (84–98 %) in differential diagnosis between AD and frontotemporal lobar degeneration.

In a recent review on imaging metrics, Frisoni et al. [1] showed a net improvement of diagnostic (AD vs healthy elderly) and prognostic accuracy (stable MCI vs prodromal MCI) with the adoption of tools such as Neurostat, t-sum, HCI and SPM in comparison with visual reading. In addition, diagnostic positive likelihood ratio (LR+) estimation showed a better differentiation between AD and HCs when adopting these metrics. As for predictive value, SPM showed the highest LR+ in differentiating between stable MCI and prodromal MCI [1]. This initial evidence supports the notion that appropriate methods of measurement increase the value of these in vivo PET techniques, making them more sensitive.

In the case of semi-quantitative methods, one should take into account several factors that might affect the results, like the correct selection of: (1) reference regions, and (2) an adequate control sample.

(a) Most semi-quantitative methods are based on scaling of reference values. This is to avoid spurious results when evaluating individuals who might present local variance in glucose consumption. This scaling can be based on the choice of a region of reference, whose values are used to scale those extracted for target regions or the whole brain. The selection of a target region (depending on the neural system studied and, subsequently, the radioligand adopted) may be challenging, given that the selected area might be also affected by pathology. Various reference regions have been proposed for ^{18}F -FDG PET imaging in AD, such as the cerebellum and sensorimotor cortex [17, 18] or pons [19]. The scaling can be also proportional, for example adjusted by global average, which is a standard procedure for SPM. This scaling adjusted by global average may be the better choice, avoiding the problem of including in the analysis an “affected” region of interest. However, there is still a lack of clear evidence about the choice of normalization methods. For example, Yakushev et al. [17] argued against scaling adjusted by global average, whereas a year later, Dukart et al. [18] suggested that global or cerebellar normalization may be used according to the study design. The authors maintained that, when differentiating dementia conditions (early AD vs early FTD), global normalization should be recommended. On the contrary, for the early diagnosis of dementia (early AD vs HC or early FTD vs HC) cerebellar normalization may be more accurate. Notably, a valid assessment of hypermetabolism relative to the controls was possible only with global normalization. These results suggest that, in the absence of clear evidence, further proof is needed to guide the selection of either global or reference region normalization approaches.

(b) The selection of an appropriate control sample is mandatory, too, given that its size and the criteria applied for establishing a normal condition may affect the results of functional and molecular PET measurements. As showed

by Mühlau et al. [20] in single-subject parametric analysis the selection of control groups of different sizes (e.g. $N = 33$ or $N = 99$) affected the sensitivity, with smaller and less numerous significant clusters being found with smaller sized comparison groups. Normality assessment criteria are also very important and are usually based on the absence of cognitive, neurological or psychiatric impairments and the use of structured interviews. Specific clinical scales like the Mini-Mental State Examination (whose score must usually be ≥ 28) or the Clinical Dementia Rating (whose score must be 0) have usually been adopted in the selection of HCs for comparison. Furthermore, for better quality results, HCs selected for comparisons should be followed up longitudinally. It has been shown that using a control group of subjects followed longitudinally for 4 years (instead of mixed databases) strongly increases the accuracy (1.4- to 2-fold) of disease detection in automated ^{18}F -FDG PET studies [21].

NeurostatTM

NeurostatTM [22–24] (University of Michigan, Ann Arbor, MI, USA) is one of the tools currently freely available online. Unlike SPM (see below), it was originally designed and developed also for single-subject analysis and is based on a routine 3D-SSP. Individual scans first undergo a stereotactic anatomical standardization based on a (non-linear) image warping along a priori stated directions of the main fiber bundles in the brain; then, the single-subject gray matter (GM) activity is projected into a pre-defined surface. The set of pre-defined voxels is then used for further statistical analysis based on the comparison between the subject and a normative reference data set. Z scores are then shown in 3D-SSP maps that can be visually evaluated. This method can also be used as a fully automated approach, setting averaged Z scores for specific regions known to be involved in the investigated disease (e.g. association cortices in AD). Users adopting this technique should be careful while evaluating the resulting 3D-SSP images, which can be affected by brain atrophy [24]. Several works in the literature have shown a high diagnostic accuracy for this method [13, 25, 26] and also a net increase in diagnostic accuracy when switching from qualitative visual interpretation to the 3D-SSP voxel-based method [13]. Foster et al., as mentioned in the introduction, evaluated the level of diagnostic accuracy when adopting ^{18}F -FDG PET 3D-SSP images rather than simple visual inspection of transaxial ^{18}F -FDG PET images in the differential diagnosis of AD versus FTD in a cohort of pathologically confirmed AD and FTD cases. The results showed an increase from 84.8 to 89.2 % in mean diagnostic accuracy in discriminating AD patients from FTD patients. Mosconi et al. [26], in a multicenter study

investigating a large cohort of patients ($N = 438$ excluding the $N = 110$ HCs), found very high diagnostic power across different clinical sample differentiation (99 % sensitivity in AD/FTD, AD/DLB and in AD/HCs). In addition, very high specificity was also found when discriminating between AD and HCs (98 % specificity), leading to an overall diagnostic accuracy of 98 %.

PALZ algorithm

The PALZ algorithm, implemented in PMOD software (PMOD Technologies, Zurich, Switzerland), is based on the initial work of Herholz et al. [10] in providing the so-called AD t -sum index. This method is based on a voxel-wise multiple t test between individual ^{18}F -FDG PET images and a reference healthy control data set, taking into account age as a nuisance variable. The index is obtained by summing the t scores belonging to a pre-defined AD-pattern mask. The original threshold proposed by Herholz et al. [10] sets an abnormality cut-off at 11.089, meaning that any subject with a t -sum >11.089 has pathological brain glucose metabolism. The validation of the method yielded high diagnostic accuracy indexes in the identification of very mild and mild-to-moderate AD patients in a large patient group ($N = 395$ probable-AD), i.e. 84 % sensitivity, 93 % specificity for the former, and 93 % sensitivity and specificity for the latter [10]. The work done by Haense et al. [27] provides another example of application of the PALZ algorithm. The authors investigated the diagnostic power of ^{18}F -FDG PET and PALZ for AD in two cohorts, belonging to the Alzheimer's Disease Neuroimaging Initiative (ADNI [28]) and to the Network for Standardization of Dementia Diagnosis (NEST-DD, [10]) for a total of $N = 326$ AD and $N = 138$ HCs. Using a preset cut-off score for detection, the authors found that (1) AD patients had a much higher AD t -sum index when compared with the HCs, and (2) early-onset AD patients had a higher t -sum index than late-onset AD patients [27]. The PALZ algorithm is very easy to use and fully automated, making it valuable in PET clinical settings. However, its utilization is bound to the PMOD commercial software. An additional limit is that the summary metrics do not provide metabolic information beyond the volume of interest.

Hypometabolism convergence index (HCI)

Initially proposed by Chen et al. [28, 29], the HCI is a very simple index consisting of a single measurement of ^{18}F -FDG distribution in a single patient compared to an average ^{18}F -FDG distribution in AD patients with hypometabolic patterns. The voxel-based algorithm of the HCI is fully automated and based on SPM. Each individual scan is

first compared with scans of normal HCs. The resulting t score (converted to z score) map is then multiplied by a vector containing the respective values from an AD z score map. The HCI is the result of this product and is designed to give more importance to higher z scores and less importance to lower z scores, to make the really significant voxels contribute to the computation of the index. The original clinical validation [29] showed the potential of HCI in identifying AD patients, MCI-stable patients or MCI converters (in 18 months) and HCs. With a cut-off point set at 8.36, HCI was the most valuable among several indexes (i.e. hippocampal volume, CSF measures, clinical and neuropsychological assessments), with an area under the curve of 0.78, in distinguishing stable patients from converters. In addition, HCI showed the greatest hazard ratio ($=7.38$) in predicting conversion to AD during the follow-up period of 18 months. Major drawbacks of the method are the lack of age-related corrections and the need for specific software (Matlab, Mathworks, Sherborn, MA, USA) and a pre-defined healthy control reference group.

Statistical parametric mapping (SPM)

Statistical parametric mapping (<http://www.fil.ion.ucl.ac.uk/spm>) procedures are, given their accessibility and power, the most widely used semi-quantitative voxel-based methods. These tools have been applied to FDG PET metabolic images both for group and single-subject analysis [8], and are widely used in both research and clinical settings for the evaluation of neurodegenerative dementia [30]. SPM is based on a pre-processing of the individual image, with smoothing and spatial normalization. The main aim of these steps is to reduce inter-subject differences and reshape individual ^{18}F -FDG PET scans to a standard normative atlas/template. Built-in templates include the standard MRI template or ^{15}O - H_2O perfusion template, but custom templates can be adopted as well. A custom ^{18}F -FDG PET template has recently been validated, yielding very promising results when used in normalization procedures [16]. This new optimized SPM method allows a significant improvement in the pre-processing phase (namely the image warping during the spatial normalization) and the application of this method to single-subject analysis [16, 31].

The main advantage of adopting the voxel-wise SPM approach is that there are no limitations to pre-defined regions of interest (ROIs); this makes it possible to detect whole-brain metabolic abnormalities. A large healthy control sample, with appropriate age- and gender-matching, is required. The resulting maps of t test comparisons (SPM- t maps) need to be evaluated by an expert, although a large body of literature reports consistent patterns in different neurodegenerative conditions. Voxel-based SPM

analysis can be very sensitive to even very mild alterations of cerebral glucose metabolism, providing SPM-t maps representing typical hypometabolic patterns that are less biased than standard qualitative visual evaluations [7, 8, 11]. This has led to the recommendation that the standard visual evaluation of FDG PET imaging should always be accompanied by a careful evaluation of SPM maps [11, 30, 32].

The amyloid PET measures

Currently, the evaluation of amyloid PET studies is most commonly based on qualitative visual assessment of the tracer accumulation in the brain by expert trained physicians [33]. In this case, the pattern and the presence of cortical tracer uptake (positive vs negative) are compared with those seen in the WM regions, where the level of tracer accumulation represents non-specific binding. The visual assessment can be rated by the physician using a score ranging from 0 (0 = no amyloid) to a maximum value (e.g. 4 = high levels of cortical amyloid) [33].

A correct qualitative evaluation of amyloid distribution is certainly easily achieved in the presence of significant amyloid deposition showing the pattern typical of AD. On the other hand, amyloid distribution is difficult to evaluate the early or preclinical AD stage, when the amyloid load is minimal and the differentiation between GM and WM uptake is not clearly evident. In these stages, it is therefore important to have available quantitative or semi-quantitative methods for an objective evaluation of the tracer uptake, to help and support the physicians in their evaluation.

In amyloid PET imaging, the use of semi-quantitative tools such as the SUVr or DVR is common, but it is recommended to carry out a proper evaluation of the adopted measure on the basis of study design and tracer properties. For example, in longitudinal studies in AD, it has been shown that the SUVr with ^{11}C -PiB compound may not be the best choice, given its high dependence on the uptake period used for the analysis of the data (40–60 min, 60–90 min) and on changes in flow. In such cases it has also been suggested to use fully quantitative analysis methods [34]. For the new-generation fluorinated amyloid tracers, on the other hand, either compartmental model binding tools like the DVR, or reference tissue model-based tools like SUVr, have provided good agreement in the discrimination between β -amyloid-positive and -negative scans and high concordance with post-mortem evaluation within 1 year of PET assessment [35]. Besides the specific method used for the analysis of the data, the selection of the reference region is also crucial for the accuracy of the results. In this regard, it has been proposed

to switch from the cerebellum to the pons as the amyloid PET reference region [36]. Future studies are clearly needed in this area.

SPM analysis

As with ^{18}F -FDG PET, some authors have adopted voxel-based measurements of amyloid PET data with SPM (or the non-parametric version of SPM for small samples), using ^{11}C -PiB [37, 38], ^{18}F -FDDNP [39] or both [39]. This approach takes advantage of several aspects, including the exploratory design of the analysis (without a priori ROIs), the ability to identify local maxima of significance, and an accurate display of the cortical tracer binding. To date, however, all the available data in the literature report group-level findings, without validation of accuracy in clinical applications to single subjects.

Distribution volume ratio (DVR)

Traditional kinetic analyses have been used for the quantitative estimation of the DVR and the binding potential (BP) of the tracer in different brain regions [40]. Analyses of this kind require the acquisition of a dynamic PET scan (e.g. 90 min) and arterial blood sampling over the duration of the study. Input function and tissue time–activity curves are then generated to be used as input data in a specific kinetic model. Alternatively, a simpler graphical analysis is sometimes adopted [40, 41]. These approaches (both for reversible and irreversible tracers) are based on descriptions of the kinetics of the radioligand in brain tissue vs plasma, which suggest a linear relationship between the two compartments after the reaching of a steady-state [40]. As regards the kinetic analysis of a reversible tracer, graphical approaches such as Logan's [42] make it possible to avoid collection of arterial blood input and yield results highly comparable with absolute quantification techniques [40]. The stable results, the optimal test/retest reliability and the correspondence to compartmental model techniques make the Logan graphical analysis the method of choice for ^{11}C -PiB. Price et al. [40] noted that Logan DVR intersubject variability in some cortical areas was lower than that reported by the compartmental method, and suggested that this variability was mostly accounted for by biological variables rather than methodological issues [40]. The Logan plot may be affected by noise-induced errors in outcome measurements, a methodological flaw that can at least partially be overcome by data smoothing [43].

The results obtained from both analyses have been shown to be effective in the discrimination between AD subjects and normal controls. On the other hand, the complexity of these PET data absolute quantifications, which require long dynamic scans and invasive arterial

blood sampling from the subject, has driven efforts to develop simpler clinical protocols. Simplified reference tissue models [44] are preferred in clinical settings where arterial input cannot be collected, and they have shown comparable results in clinical diagnosis [41].

As a matter of fact, as shown by Wong et al. [45] in relation to ^{18}F -labeled PET β -amyloid imaging tracer, the cortical-to-cerebellar activity ratio in AD patients increased continuously for 30 min after tracer administration, reaching a plateau within 50 min and then remaining stable until at least 90 min post-injection. On the basis of these results, a 10-min static PET scan from 50 to 60 min after tracer administration was recommended for clinical use [45].

Standard uptake value ratio

A simple semi-quantitative data analysis, in which the SUVr has been proposed as the index ratio for evaluation of the cortical amyloid burden, provides the basis of a simplified acquisition protocol. The SUVr is defined as the ratio between the standard uptake values (SUVs) measured in ROIs positioned on cortical regions, and those measured in ROIs on the cerebellar cortex or the whole cerebellum, a region in which tracer uptake is consistently low [45, 46]. Besides the cerebellum, other brain regions like the pons or centrum semiovale have also been used as reference regions for calculation of the SUVr [36, 45, 46].

Other approaches for the extraction of more accurate reference regions, like clustering techniques, are currently a topic of research interest. For example, Ikoma et al. [47] recently validated a three-class clustering technique for the automatic extraction of the best reference region in dynamic ^{11}C -PiB PET brain studies in a sample of familial AD patients.

The SUVr can be calculated directly on the original PET images or, as shown by Fleisher et al. [46], on PET images once these have been normalized into a standard template (the Montreal Neurological Institute atlas) using SPM software. It is to be noted that, depending on the amyloid radioligand adopted (^{11}C -PiB or fluorinated tracers such as ^{18}F -flutemetamol), the SUVr may yield inconsistent results and/or overestimations [34, 41, 48]. It has recently been shown that ^{11}C -PiB SUVr measures in longitudinal studies may be flow dependent and may overestimate the specific binding of the tracer, suggesting that it may be opportune to adopt other measures like Logan DVRs [34].

Overall, semi-quantitative or quantitative measures require thresholds for positivity/negativity. Thresholds need to be set versus a pathological gold standard, equalized across different ligands, and include information on the risk of developing dementia for sub-threshold degrees of amyloid positivity.

Partial volume effects (PVEs): compensation techniques

Regardless of the specific evaluation strategy chosen for the analysis of amyloid load, the general aims are (1) to improve, qualitatively, the visual contrast between the tracer accumulation in the GM and WM, and (2) to improve, quantitatively, the accuracy of the estimation of the radioactivity distribution in the GM and WM. Unfortunately, in both cases such evaluations can be affected by the poor spatial resolution (SR) of PET. In fact, even with state-of-the-art PET/CT or PET/MR scanners, the SR of PET is relatively low (4–6 mm) in comparison with that of anatomical/structural imaging techniques like CT or MRI. The finite SR of PET produces a spread of the activity distribution, which becomes mixed with the contribution of neighboring tissues, resulting in confounding effects, also called PVEs [49, 50].

From the qualitative point of view, PVEs result in degradation of the image quality, which reduces the image contrast between different types of tissue (e.g. GM and WM), while from the quantitative point of view, they produce a bias in estimates of regional radioactivity concentration. PVEs become particularly important when the source of interest (target) is smaller than <2 – 3 the full width at half maximum of the system's point spread function. Considering that the size of nearly all brain structures is <2 – 3 the SR of the PET scanner (i.e. the GM thickness is about 2.5 mm), it is easy to understand the importance of improving SR and the need to compensate for PVEs to obtain accurate quantitative PET estimates of amyloid deposition in the cortical regions (cf. among others, [49, 51, 52]). Furthermore, as is well known, PVEs can play an important role in the evaluation of those neurodegenerative diseases characterized by progressive atrophy with consequent reduction/loss of GM. In such cases, PVEs result in a global reduction of the PET signal. To discriminate whether such a reduction is due to the presence of atrophy or, instead, represents a real functional tissue reduction, PVE compensation is needed. PVE correction techniques could thus represent an important tool for improving, both qualitatively and quantitatively, the analysis of PET brain images by removing, or at least reducing, the confounding effects caused by the poor SR of PET.

Several techniques have been developed over the years for recovery of SR and PVE correction in PET brain studies. Most of these methods use spatially co-registered high-resolution anatomical images serving to support the SR recovery as well as the PVE correction techniques. One early study by Videen et al. [53] aimed specifically to correct for the PVEs caused by cerebral atrophy. As Videen's method did not allow for PVE compensation between brain structures with high and low activity (e.g. GM and WM), an improvement of the technique was

subsequently proposed by Müller-Gärtner et al. [54] (MG). The MG method requires segmentation of the magnetic resonance images into three binary maps representing the distribution of the GM, the WM and the cerebrospinal fluid (CSF). The method assumes that the radioactivity concentration in WM and CSF is constant and known. The technique is based on the subtraction from the observed (degraded) PET images of the contributions of WM and CSF images degraded by the PSF. The resulting images should thus be representative of PET image degradation due to GM only. The final division (pixel by pixel) of these degraded GM images by that resulting from the convolution of the GM (binary map) with the PSF generates the GM PVE-corrected images. Even though the MG method allows corrections for GM PVEs, it may incompletely correct GM structures when local tissue concentrations are highly heterogeneous.

To account for these situations Meltzer et al. [55] extended the original MG model to a fourth compartment (namely a volume of interest—VOI in the GM, the mean value of which is different from that of the remaining GM). Notwithstanding this extension of the MG method to account for heterogeneity in the GM tissue, the PVE correction is valid only for the two considered target regions (i.e. GM and VOI). To overcome this limitation, Yang et al. [56] proposed a new method allowing the production of a PVE-corrected image over multiple ROIs.

Other techniques that allow the analysis to be performed over multiple ROIs are those referred to as partition methods. One of the most popular is the geometric transfer matrix (GTM) method, proposed by Rousset et al. [51]. Unlike the previously described approaches, the GTM technique is a region-based algorithm that uses anatomical data from an MR scan to perform PVE correction on PET images over multiple ROIs. In particular, the technique requires that a set of spatially co-registered MR images be subdivided into a set of non-overlapping ROIs in which uniform radioactivity distribution is assumed. The PVE effect between any possible pair of ROIs is accounted for by a matrix (GTM) of coefficients, referred to as regional response functions. Knowing the PET values for each ROI and the GTM, a system of linear equations can be built, the solution of which provides the true radioactivity value (PVE corrected) for each ROI. More recently, Thomas et al. [57] proposed a new technique called region-based voxel-wise (RBV) PVE correction. The RBV technique extends the GTM method, in that it combines a region-based method (the GTM) with a voxel-wise correction over the entire image (the Yang method). As a matter of fact, the first step of the RBV method requires the subdivision of the anatomical images into a set of non-overlapping ROIs, which are used to run the GTM method. Once the GTM-corrected values for each of the different ROIs have been

obtained the second step consists of a voxel-wise correction procedure over the whole image, which is performed using the Yang approach.

A different methodology aiming to recover the SR and to perform PVE correction through the generation of new PVE-corrected images was proposed by Boussion et al. [58]. The method is a functional–anatomical post-processing technique that uses wavelet transform and multi-resolution analysis. In this method, the core of the technique is to transfer the spatial frequencies, characterizing high-resolution spatial details from the high-resolution (CT or MR) anatomical images to the low-resolution (PET) functional images, to improve both image quality and quantitative accuracy of PET images.

All the above methods have given good results, but require the availability of the spatially co-registered anatomical data (in particular, an MR image), and in several cases also need the segmentation of these data to be used in the correction technique. This requirement can represent a limitation as regards the clinical application of these correction techniques and, furthermore, makes their accuracy dependent on the segmentation algorithm used. To avoid such dependence, different techniques, based on image reconstruction or image post-processing, have been developed to improve the SR and thus reduce the PVEs. These techniques demand knowledge of the PSF of the PET scanner, which is directly incorporated in the reconstruction scheme [59–61] or accounted for in specific post-processing restoration techniques (image deconvolution) [62–64]. In both cases no anatomical information is needed, and this represents a degree of freedom for these methods. On the other hand, both image reconstruction and image deconvolution techniques suffer from a common problem, namely the increase of the noise generated by the SR recovery process.

As can be easily understood, each of these correction techniques has specific advantages and disadvantages. It is thus important to be aware of such specificities when adopting one of these techniques for clinical applications [57].

On the other hand, the weaknesses of the SR recovery and PVE correction techniques will be reduced by the continuous technological evolution of both hardware and software. In fact, the introduction of hybrid fully integrated PET/MRI systems should make an important contribution, particularly as regards neurological applications, to the significant improvement, both qualitative and quantitative, of PET images. The simultaneity of the PET and MRI acquisitions should remove the co-registration problems, while new dedicated MRI sequences will improve the signal-to-noise ratio (SNR) and thus the accuracy of the resulting MRI segmentation. As regards PET/CT, a new detector design combining smaller crystals coupled with

fully digital signal technology and powerful time-of-flight capability (e.g. <300 ps) is expected to significantly improve the SR and the SNR of the PET signal. Notwithstanding all these technological advances, the SR of clinical whole-body PET systems will remain “poor” (e.g. 2–3 mm) due to the intrinsic limitations of the technique itself (positron range, non-collinearity, detector dimensions, detector arrangement, etc.) and thus SR recovery/PVE compensation techniques will continue to be needed.

Conclusions

Biomarkers of brain amyloidosis and neurodegeneration/synaptic dysfunction are featured in the most recent diagnostic criteria for AD and other dementia conditions. Correct evaluation of both cerebral glucose metabolism and β -amyloid burden is fundamentally important for early and differential diagnosis of dementia. The ability to detect a disease process even before the occurrence of clinical manifestations, together with the ability to discriminate between different neurodegenerative conditions, has huge implications for diagnostic imaging in research, clinical trials and future therapeutic approaches.

In the case of cerebral glucose metabolism, a large amount of literature has provided clear evidence of specific, disease-related ^{18}F -FDG PET patterns [30, 65–67], which are significantly accurate and useful for differential diagnosis. More specifically, a temporoparietal hypometabolism (as resulting from comparison with healthy controls) is considered a hallmark of AD. Its detection is thus crucial in clinical settings. The value of amyloid PET in clinical settings remains to be defined. Among the factors to be considered are its lack of correlation with cognitive status and neuronal injury biomarkers and its low performance in predicting progression or differentiating between subtypes of MCI [68]. Amyloid PET is only a marker of amyloid pathology *in vivo* and lacks diagnostic power in differentiating between different AD variants, DLB and cerebral amyloid angiopathy [69, 70]. Nonetheless, there are several clinical situations in which amyloid PET has a crucial role, for example in early-onset atypical presentations and in the primary progressive aphasia spectrum (e.g. logopenic variant vs non-fluent). More generally, a negative amyloid scan has been shown to effectively rule out AD [12, 71].

Nowadays, the main applications are no longer limited to the diagnosis of early and clinically manifest AD, and are also extending towards the definition of the preclinical stages of AD. PET molecular techniques can detect specific disease processes in single individuals at asymptomatic AD stages, when there is no evidence of anatomical changes on CT and MRI. ^{18}F -FDG PET and amyloid PET have high

power in detecting biological changes in prodromal and even preclinical AD stages, not only in at-risk individuals but also in sporadic AD conditions [72–74].

AD is a slowly progressive disorder in which pathophysiological abnormalities precede overt clinical symptoms by many years to decades, as shown *in vivo* by PET biomarkers in at-risk individuals and also in healthy subjects with ApoE (both E4+ and E4–) and subjective memory complaints. Recently, the amyloid cascade hypothesis in AD has been revised, suggesting that neurodegenerative mechanisms like synaptic loss and/or dysfunction, which are detected by ^{18}F -FDG PET, are early pathological events that can be distinct from β -amyloid deposition in the brain (see [75]).

The diagnostic accuracy of PET neuroimaging greatly depends on the use of semi-quantitative methods [1, 9, 11]; therefore, to achieve solid diagnostic results, researchers and physicians need to adopt appropriate metrics when analyzing PET data.

As regards their clinical use, ^{18}F -FDG PET scans were traditionally mainly used in qualitative visual interpretation of the images; however, they are now increasingly being used in voxel-based and automatic procedures for the measurement of hypometabolism. Sensitive and specific ^{18}F -FDG PET analysis tools for the detection of brain functional derangement are crucial, particularly for the detection of early metabolic changes associated with specific cognitive symptoms (i.e. early diagnosis). Visual inspection of an ^{18}F -FDG PET image is hampered by the lack of clear-cut features distinguishing between a normal and a pathological scan, and only methods employing parametric and voxel-based analysis techniques can provide unbiased, statistically defined measures of brain abnormality across the whole brain.

Since the development of new criteria for the *in vivo* diagnosis of AD and other neurodegenerative dementia conditions [2, 76–79], standardization and the development of cost-effective measures of “core” neuroimaging biomarkers for differential and early diagnosis in the clinic have become the steps that need to be implemented. The standardization of biomarkers, which is still incomplete, should be carried out particularly in memory clinics that have demonstrated capability to collect and measure biomarkers with the highest current operational standards. To achieve standardization of voxel-based mapping tools and summary metrics of ^{18}F -FDG PET brain hypometabolism, as well as of SUVRs and DVRs for the amyloid load with PET imaging, the following are needed: (1) internationally recognized control data sets (e.g. US ADNI, NEST-DD or the European Alzheimer’s Disease PET Consortium—EADC-PET) that include individuals who are neuropsychologically well characterized and can be followed up for a few years to exclude progressive cognitive deterioration

(these normal data sets should be sufficiently large to allow stable estimates of accuracy and of the effects of clinical covariates); (2) pathological cases that are representative of the clinical population studied; (3) validation and use of ad hoc templates for spatial normalization [16]; (4) definition of sensitivity and specificity to the typical hypometabolic patterns obtained with the different tools; (5) definition of minimum diagnostic and prognostic performance metrics for new analysis methods based on benchmarks. The standardization of PET procedures is mandatory to obtain optimized protocols for PET imaging interpretation in neurology.

Finally, it is hoped that effective disease-modifying treatments will arise from strategies addressing the early and preclinical stages of dementia. Improved knowledge of the chain of events leading from synaptic dysfunction and neurodegeneration, to deposition of A β and phosphorylated tau, up to AD symptoms is crucial for developing drugs aiming at slowing or preventing AD. The most promising contemporary diagnostic strategies involve the performance of high-level diagnostic imaging using advanced PET technologies and validated metrics.

Conflict of interest The authors (Perani D, Iaccarino L, Bettinardi V) declare that they have no conflicts of interest to report regarding this article.

Human and animal studies This article does not contain any studies with human or animal subjects performed by the any of the authors.

References

- Frisoni GB, Bocchetta M, Chételat G, Rabinovici GD, de Leon MJ, Kaye J et al (2013) Imaging markers for Alzheimer disease: which vs how. *Neurology* 81:487–500
- Dubois B, Feldman HH, Jacova C, DeKosky ST, Barberger-Gateau P, Cummings J et al (2007) Research criteria for the diagnosis of Alzheimer's disease: revising the NINCDS-ADRDA criteria. *Lancet Neurol* 6:734–746
- Jack CR Jr, Albert MS, Knopman DS, McKhann GM, Sperling RA, Carrillo MC et al (2011) Introduction to the recommendations from the National Institute on Aging-Alzheimer's Association workgroups on diagnostic guidelines for Alzheimer's disease. *Alzheimers Dement* 7:257–262
- Prestia A, Caroli A, van der Flier WM, Ossenkoppele R, Van Berckel B, Barkhof F et al (2013) Prediction of dementia in MCI patients based on core diagnostic markers for Alzheimer disease. *Neurology* 80:1048–1056
- Jack CR Jr, Holtzman DM (2013) Biomarker modeling of Alzheimer's disease. *Neuron* 80:1347–1358
- Waxman AD, Herholz K, Lewis DH, Herscovitch P, Minoshima S, Mountz JM et al (2009) Society of nuclear medicine procedure guideline for FDG PET brain imaging. Version 1.0
- Anchisi D, Borroni B, Franceschi M, Kerrouche N, Kalbe E, Beuthien-Beumann B et al (2005) Heterogeneity of brain glucose metabolism in mild cognitive impairment and clinical progression to Alzheimer disease. *Arch Neurol* 62:1728–1733
- Signorini M, Paulesu E, Friston K, Perani D, Colleluori A, Lucignani G et al (1999) Rapid assessment of regional cerebral metabolic abnormalities in single subjects with quantitative and nonquantitative [18 F]FDG PET: a clinical validation of statistical parametric mapping. *Neuroimage* 9:63–80
- Caroli A, Prestia A, Chen K, Ayutyanont N, Landau SM, Madison CM et al (2012) Summary metrics to assess Alzheimer disease-related hypometabolic pattern with 18 F-FDG PET: head-to-head comparison. *J Nucl Med* 53:592–600
- Herholz K, Salmon E, Perani D, Baron J-C, Holthoff V, Frölich L et al (2002) Discrimination between Alzheimer dementia and controls by automated analysis of multicenter FDG PET. *Neuroimage* 17:302–316
- Perani D, Schillaci O, Padovani A, Nobili FM, Iaccarino L, Della Rosa PA et al (2014) A survey of FDG and amyloid PET imaging in dementia and GRADE analysis. *Biomed Res Int*. doi:10.1155/2014/785039
- Vandenberghe R, Adamczuk K, Dupont P, Van Laere K, Chételat G (2013) Amyloid PET in clinical practice: its place in the multidimensional space of Alzheimer's disease. *Neuroimage Clin* 2:497–511
- Foster NL, Heidebrink JL, Clark CM, Jagust WJ, Arnold SE, Barbas NR et al (2007) FDG-PET improves accuracy in distinguishing frontotemporal dementia and Alzheimer's disease. *Brain* 130:2616–2635
- Patterson JC, Lilien DL, Takalkar A, Pinkston JB (2011) Early detection of brain pathology suggestive of early AD using objective evaluation of FDG-PET scans. *Int J Alzheimers Dis*. doi:10.4061/2011/946590
- Rabinovici GD, Rosen HJ, Alkalay A, Kornak J, Furst AJ, Agarwal N et al (2011) Amyloid vs FDG-PET in the differential diagnosis of AD and FTL. *Neurology* 77:2034–2042
- Della Rosa PA, Cerami C, Gallivanone F, Prestia A, Caroli A, Castiglioni I, Gilardi MC et al (2014) A standardized [18 F]-FDG-PET template for spatial normalization in statistical parametric mapping of dementia. *Neuroinformatics* [Epub ahead of print]
- Yakushev I, Hammers A, Fellgiebel A, Schmidtman I, Scheurich A, Buchholz H-G et al (2009) SPM-based count normalization provides excellent discrimination of mild Alzheimer's disease and amnesic mild cognitive impairment from healthy aging. *Neuroimage* 44:43–50
- Dukart J, Mueller K, Horstmann A, Vogt B, Frisch S, Barthel H et al (2010) Differential effects of global and cerebellar normalization on detection and differentiation of dementia in FDG-PET studies. *Neuroimage* 49:1490–1495
- Minoshima S, Frey KA, Foster NL, Kuhl DE (1995) Preserved pontine glucose metabolism in Alzheimer disease: a reference region for functional brain image (PET) analysis. *J Comput Assist Tomogr* 19:541–547
- Muhlau M, Wohlschlagel AM, Gaser C, Valet M, Weindl A, Nunnemann S et al (2009) Voxel-based morphometry in individual patients: a pilot study in early Huntington disease. *AJNR Am J Neuroradiol* 30:539–543
- Mosconi L, Tsui WH, Pupi A, De Santi S, Drzezga A, Minoshima S et al (2007) 18F-FDG PET database of longitudinally confirmed healthy elderly individuals improves detection of mild cognitive impairment and Alzheimer's disease. *J Nucl Med* 48:1129–1134
- Minoshima S, Koeppe RA, Frey KA, Kuhl DE (1994) Anatomic standardization: linear scaling and nonlinear warping of functional brain images. *J Nucl Med* 35:1528–1537
- Minoshima S, Frey KA, Koeppe RA, Foster NL, Kuhl DE (1995) A diagnostic approach in Alzheimer's disease using three-dimensional stereotactic surface projections of fluorine-18-FDG PET. *J Nucl Med* 36:1238–1248
- Ishii K, Willoch F, Minoshima S, Drzezga A, Ficarò EP, Cross DJ et al (2001) Statistical brain mapping of 18 F-FDG PET in

- Alzheimer's disease: validation of anatomic standardization for atrophied brains. *J Nucl Med* 42:548–557
25. Minoshima S, Foster NL, Sima AA, Frey KA, Albin RL, Kuhl DE (2001) Alzheimer's disease versus dementia with Lewy bodies: cerebral metabolic distinction with autopsy confirmation. *Ann Neurol* 50:358–365
 26. Mosconi L, Tsui WH, Herholz K, Pupi A, Drzezga A, Lucignani G et al (2008) Multicenter standardized ¹⁸F-FDG PET diagnosis of mild cognitive impairment, Alzheimer's disease, and other dementias. *J Nucl Med* 49:390–398
 27. Haense C, Herholz K, Jagust WJ, Heiss WD (2009) Performance of FDG PET for detection of Alzheimer's disease in two independent multicentre samples (NEST-DD and ADNI). *Dement Geriatr Cogn Disord* 28:259–266
 28. Jagust WJ, Bandy D, Chen K, Foster NL, Landau SM, Mathis CA et al (2010) The Alzheimer's disease neuroimaging initiative positron emission tomography core. *Alzheimers Dement* 6:221–229
 29. Chen K, Ayutyanont N, Langbaum JBS, Fleisher AS, Reschke C, Lee W et al (2011) Characterizing Alzheimer's disease using a hypometabolic convergence index. *Neuroimage* 56:52–60
 30. Perani D (2013) FDG PET and cognitive symptoms of dementia. *Clin Transl Imaging* 1:247–260
 31. Della Rosa PA, Cerami C, Prestia A, Gallivanone F, Frisoni G, Nobili F et al (2012) Clinical validation of a grid-based SPM web tool for the automatic assessment of [¹⁸F]FDG PET brain metabolic abnormalities in single subjects. *Neurology (Meeting Abstracts)*. Dec. 13:P03.106
 32. Otte A, Halsband U (2006) Brain imaging tools in neurosciences. *J Physiol Paris* 99:281–292
 33. Clark CM, Schneider JA, Bedell BJ, Beach TG, Bilker WB, Mintun MA et al (2011) Use of florbetapir-PET for imaging beta-amyloid pathology. *JAMA* 305:275–283
 34. van Berckel BNM, Ossenkoppele R, Tolboom N, Yaqub M, Foster-Dingley JC, Windhorst AD et al (2013) Longitudinal amyloid imaging using ¹¹C-PiB: methodologic considerations. *J Nucl Med* 54:1570–1576
 35. Becker GA, Ichise M, Barthel H, Luthardt J, Patt M, Seese A et al (2013) PET quantification of ¹⁸F-florbetaben binding to β-amyloid deposits in human brains. *J Nucl Med* 54:723–731
 36. Edison P, Hinz R, Ramlackhansingh A, Thomas J, Gelosa G, Archer HA et al (2012) Can target-to-pons ratio be used as a reliable method for the analysis of [¹¹C]PIB brain scans? *Neuroimage* 60:1716–1723
 37. Ziolk SK, Weissfeld LA, Klunk WE, Mathis CA, Hoge JA, Lopresti BJ et al (2006) Evaluation of voxel-based methods for the statistical analysis of PIB PET amyloid imaging studies in Alzheimer's disease. *Neuroimage* 33:94–102
 38. Kempainen NM, Aalto S, Wilson IA, Nägren K, Helin S, Brück A et al (2006) Voxel-based analysis of PET amyloid ligand [¹¹C]PIB uptake in Alzheimer disease. *Neurology* 67:1575–1580
 39. Shin J, Lee S-Y, Kim S-H, Kim Y-B, Cho S-J (2008) Multitracer PET imaging of amyloid plaques and neurofibrillary tangles in Alzheimer's disease. *Neuroimage* 43:236–244
 40. Price JC, Klunk WE, Lopresti BJ, Lu X, Hoge JA, Ziolk SK et al (2005) Kinetic modeling of amyloid binding in humans using PET imaging and Pittsburgh Compound-B. *J Cereb Blood Flow Metab* 25:1528–1547
 41. Lopresti BJ, Klunk WE, Mathis CA, Hoge JA, Ziolk SK, Lu X et al (2005) Simplified quantification of Pittsburgh Compound B amyloid imaging PET studies: a comparative analysis. *J Nucl Med* 46:1959–1972
 42. Logan J (2000) Graphical analysis of PET data applied to reversible and irreversible tracers. *Nucl Med Biol* 27:661–670
 43. Logan J, Fowler JS, Volkow ND, Ding YS, Wang GJ, Alexoff DL (2001) A strategy for removing the bias in the graphical analysis method. *J Cereb Blood Flow Metab* 21:307–320
 44. Yaqub M, Tolboom N, Boellaard R, van Berckel BNM, van Tilburg EW, Luurtsema G et al (2008) Simplified parametric methods for [¹¹C]PIB studies. *Neuroimage* 42:76–86
 45. Wong DF, Rosenberg PB, Zhou Y, Kumar A, Raymont V, Ravert HT et al (2010) In vivo imaging of amyloid deposition in Alzheimer disease using the radioligand ¹⁸F-AV-45 (florbetapir F 18). *J Nucl Med* 51:913–920
 46. Fleisher AS, Chen K, Liu X, Roontiva A, Thiyyagura P, Ayutyanont N et al (2011) Using positron emission tomography and florbetapir F 18 to image cortical amyloid in patients with mild cognitive impairment or dementia due to Alzheimer disease. *Arch Neurol* 68:1404–1411
 47. Ikoma Y, Edison P, Ramlackhansingh A, Brooks DJ, Turkheimer FE (2013) Reference region automatic extraction in dynamic [¹¹C]PIB. *J Cereb Blood Flow Metab* 33:1725–1731
 48. Nelissen N, Van Laere K, Thurfjell L, Owenius R, Vandenbulcke M, Koole M et al (2009) Phase I study of the Pittsburgh compound B derivative ¹⁸F-flutemetamol in healthy volunteers and patients with probable Alzheimer disease. *J Nucl Med* 50:1251–1259
 49. Hoffman EJ, Huang SC, Phelps ME (1979) Quantitation in positron emission computed tomography: 1. Effect of object size. *J Comput Assist Tomogr* 3:299–308
 50. Kessler RM, Ellis JR, Eden M (1984) Analysis of emission tomographic scan data: limitations imposed by resolution and background. *J Comput Assist Tomogr* 8:514–522
 51. Rousset OG, Ma Y, Evans AC (1998) Correction for partial volume effects in PET: principle and validation. *J Nucl Med* 39:904–911
 52. Hoetjes NJ, van Velden FHP, Hoekstra OS, Hoekstra CJ, Krak NC, Lammertsma AA et al (2010) Partial volume correction strategies for quantitative FDG PET in oncology. *Eur J Nucl Med Mol Imaging* 37:1679–1687
 53. Videen TO, Perlmutter JS, Mintun MA, Raichle ME (1988) Regional correction of positron emission tomography data for the effects of cerebral atrophy. *J Cereb Blood Flow Metab* 8:662–670
 54. Muller-Gartner HW, Links JM, Prince JL, Bryan RN, McVeigh E, Leal JP et al (1992) Measurement of radiotracer concentration in brain gray matter using positron emission tomography: MRI-based correction for partial volume effects. *J Cereb Blood Flow Metab* 12:571–583
 55. Meltzer CC, Zubieta J-K, Links JM, Brakeman P, Stumpf MJ, Frost JJ (1996) MR-based correction of brain PET measurements for heterogeneous gray matter radioactivity distribution. *J Cereb Blood Flow Metab* 16:650–658
 56. Yang J, Huang S, Mega M, Lin K, Toga A, Small G et al (1996) Investigation of partial volume correction methods for brain FDG PET studies. *IEEE Trans Nucl Sci* 43:3322–3327
 57. Thomas BA, Erlandsson K, Modat M, Thurfjell L, Vandenberghe R, Ourselin S et al (2011) The importance of appropriate partial volume correction for PET quantification in Alzheimer's disease. *Eur J Nucl Med Mol Imaging* 38:1104–1119
 58. Boussion N, Chez Le Rest C, Hatt M, Visvikis D (2009) Incorporation of wavelet-based denoising in iterative deconvolution for partial volume correction in whole-body PET imaging. *Eur J Nucl Med Mol Imaging* 36:1064–1075
 59. Alessio AM, Stearns CW, Tong S, Ross SG, Kohlmyer S, Ganin A et al (2010) Application and evaluation of a measured spatially variant system model for PET image reconstruction. *IEEE Trans Med Imaging* 29:938–949
 60. Panin VY, Kehren F, Michel C, Casey M (2006) Fully 3-D PET reconstruction with system matrix derived from point source measurements. *IEEE Trans Med Imaging* 25:907–921
 61. Reader AJ, Julyan PJ, Williams H, Hastings DL, Zweit J (2003) EM algorithm system modeling by image-space techniques for PET reconstruction. *IEEE Trans Nucl Sci* 50:1392–1397

62. Teo BK, Seo Y, Bacharach SL, Carrasquillo JA, Libutti SK, Shukla H et al (2007) Partial-volume correction in PET: validation of an iterative postreconstruction method with phantom and patient data. *J Nucl Med* 48:802–810
63. Tohka J, Reilhac A (2008) Deconvolution-based partial volume correction in Raclopride-PET and Monte Carlo comparison to MR-based method. *Neuroimage* 39:1570–1584
64. Kirov A, Piao J, Schmidtlein C (2008) Partial volume effect correction in PET using regularized iterative deconvolution with variance control based on local topology. *Phys Med Biol* 53:2577–2591
65. Perani D (2008) Functional neuroimaging of cognition. *Handb Clin Neurol* 88:61–111
66. Teune LK, Bartels AL, de Jong BM, Willemsen ATM, Eshuis SA, de Vries JJ et al (2010) Typical cerebral metabolic patterns in neurodegenerative brain diseases. *Mov Disord* 25:2395–2404
67. Berti V, Pupi A, Mosconi L (2011) PET/CT in diagnosis of dementia. *Ann NY Acad Sci* 1228:81–92
68. Vandenberghe R, Adamczuk K, Van Laere K (2013) The interest of amyloid PET imaging in the diagnosis of Alzheimer's disease. *Curr Opin Neurol* 26:646–655
69. Laforce R, Rabinovici GD (2011) Amyloid imaging in the differential diagnosis of dementia: review and potential clinical applications. *Alzheimers Res Ther* 3:31
70. Lehmann M, Ghosh PM, Madison C, Laforce R, Corbetta-Rastelli C, Weiner MW et al (2013) Diverging patterns of amyloid deposition and hypometabolism in clinical variants of probable Alzheimer's disease. *Brain* 136:844–858
71. Johnson KA, Minoshima S, Bohnen NI, Donohoe KJ, Foster NL, Herscovitch P et al (2013) Update on appropriate use criteria for amyloid PET imaging: dementia experts, mild cognitive impairment, and education. *Alzheimers Dement* 9:e106–e109
72. Mosconi L, Murray J, Tsui WH, Li Y, Spector N, Goldowsky A et al (2014) Brain imaging of cognitively normal individuals with 2 parents affected by late-onset AD. *Neurology* 82:752–760
73. Johnson SC, Christian BT, Okonkwo OC, Oh JM, Harding S, Xu G et al (2014) Amyloid burden and neural function in people at risk for Alzheimer's disease. *Neurobiol Aging* 35:576–584
74. Vos SJ, Xiong C, Visser PJ, Jasielec MS, Hassenstab J, Grant EA et al (2013) Preclinical Alzheimer's disease and its outcome: a longitudinal cohort study. *Lancet Neurol* 12:957–965
75. Perani D (2014) FDG-PET and amyloid-PET imaging: the diverging paths. *Curr Opin Neurol* 27:405–413
76. McKeith IG, Dickson DW, Lowe J, Emre M, O'Brien JT, Feldman H et al (2005) Diagnosis and management of dementia with Lewy bodies: third report of the DLB Consortium. *Neurology* 65:1863–1872
77. Rascovsky K, Hodges JR, Knopman D, Mendez MF, Kramer JH, Neuhaus J et al (2011) Sensitivity of revised diagnostic criteria for the behavioural variant of frontotemporal dementia. *Brain* 134(Pt 9):2456–2477
78. Dubois B, Feldman HH, Jacova C, Cummings JL, DeKosky ST, Barberger-Gateau P et al (2010) Revising the definition of Alzheimer's disease: a new lexicon. *Lancet Neurol* 9:1118–1127
79. McKhann GM, Knopman DS, Chertkow H, Hyman BT, Jack CR Jr, Kawas CH et al (2011) The diagnosis of dementia due to Alzheimer's disease: recommendations from the National Institute on Aging-Alzheimer's Association workgroups on diagnostic guidelines for Alzheimer's disease. *Alzheimers Dement* 7:263–269